GLOBAL ACADEMIC RESEARCH INSTITUTE

COLOMBO, SRI LANKA

GARI International Journal of Multidisciplinary Research

ISSN 2659-2193

Volume: 08 | Issue: 03

On 30th September 2022

http://www.research.lk

Author: Triffina Amaratunga, Dr. Mathi Kandiah, Sandali Abhaywardena

School of Science, BMS, Sri Lanka

GARI Publisher | Nanotechnology | Volume: 08 | Issue: 03

Article ID: IN/GARI/ICAS/2022/116 | Pages: 109-130 (22)

ISSN 2659-2193 | Edit: GARI Editorial Team

Received: 15.07.2022 | Publish: 30.09.2022

GREEN SYNTHESIS OF SILVER NANOPARTICLES USING SIX VARIETIES OF HIBISCUS ROSA-SINENSIS LEAF EXTRACTS: EVALUATION OF ANTIOXIDANT ACTIVITY, ANTIBACTERIAL ACTIVITY AND PHOTOCATALYTIC PROPERTIES

Triffina Amaratunga, Dr. Mathi Kandiah, Sandali Abhaywardena

School of Science, BMS, Sri Lanka

ABSTRACT

The production of nanomaterials through nanotechnology has aided in the advancement of healthcare and therapy. Silver nanoparticles (AgNPs) are being employed in a variety of fields, due to their distinctive chemical and physical characteristics. The present study endeavours the eco-friendly green synthesis of AgNPs from six varieties of the medicinally significant 'Hibiscus rosa-sinensis' leaves to determine its antioxidant, antimicrobial, and photocatalytic properties. The extraction procedure was conducted using water. 1mL of water extract was mixed with 9mL of silver nitrate and was optimized at 90℃ for 60 minutes to gain nanoparticles. The colour change from colourless to brown and the absorption peak obtained between 400-480nm using UV-Vis spectrophotometer, indicated the formation of AgNPs. The occurrence of the peak is due to the Surface Plasmon Resonance phenomenon. The synthesized yellow AgNPs were characterized using Scanning Electron Microscopy and it was observed that yellow AgNPs were spherical in shape and 50nm in size. Synthesized AgNPs showed higher antioxidant activity by showing a positive correlation between the Total Flavonoid Content, Total Phenolic Content, and Total Antioxidant Content assays conducted. All synthesized AgNPs were categorized as semiconductors based on the calculated bandgap energies. The antibacterial activity of AgNPs and water extracts were investigated against Escherichia coli and Staphylococcus aureus. Yellow AgNPs had a higher inhibition zone against S. aureus compared to E. coli. Photocatalytic activity of yellow AgNPs was measured using Methyl Orange. 267ppm yellow AgNPs exhibited a higher degradation by completely degrading within 60 minutes with a rate constant of 0.1048 whereas, the 4000ppm yellow AgNPs required 90 minutes. The results imply that hibiscus has the potential to develop new medicines that help to lessen various free radical-induced diseases due to its high antioxidant and antimicrobial activity.

Keywords: Nanotechnology, Silver nanoparticles, Hibiscus rosa-sinensis

INTRODUCTION

Nanotechnology is a broad term that encompasses a variety of scientific, research, and technological fields. Nanotechnology is defined as “research and technology development at the atomic, molecular or macromolecular levels in the length of approximately 1-100nm” (Madkour, 2019). Nanomaterials have unique physical and chemical features that can be used for societal applications such as biomedicine and drug delivery, food and agriculture, paints and cosmetics, and electronics (Nasrollahzadeh et al., 2019).

In order to obtain nanomaterials of appropriate sizes, shapes, and functions, two distinct fundamental principles of synthesis have been approached which are top-down and bottom-up methods (Figure 1). The top-down method starts with large bulky material and brought it down to nanoscale whereas, the bottom-up approach involves joining atoms and molecules and growing them into a large complex structure by using nanoscale chemical or physical forces. Hence, in bottom-up approach size reduction was done conventionally by using a variety of toxic materials that are potentially harmful to the environment. Thus, to eliminate these adverse effects and counter the other limitations such as lack of understanding of fundamental mechanisms and high expenses, a new era of "green synthesis" has gained great attention (Singh et al., 2018).

Green synthesis of nanomaterials is the production of various nanoparticles employing bioactive agents such as diverse bio-wastes, plant materials, and microorganisms (Figure 1). Since plants are non-pathogenic and readily available with a least cost, they are predominantly used for the green synthesis of nanoparticles than microbes (Zhang et al., 2020). Green synthesis avoids the production of unwanted harmful toxic products through eco-friendly synthetic procedures. This method is cost-effective, has less energy requirements, and can be used at the large-scale production of nanoparticles (Singh et al., 2018). Nanoparticles synthesized from metals are popular these days due to their various applications in biology and medicine. Among them, AgNP is an interesting nanometal due to its unique

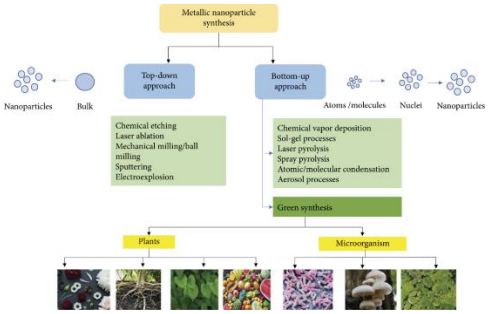

Figure 1: Synthetic approaches of Nanotechnology (Kandiah and Chandrasekaran, 2018)

characteristics which include high antibacterial activity, localized surface plasmon resonance, high conductivity, catalytic activity, and less toxicity (Fairuzi et al., 2018).

When synthesizing AgNPs, the metal ions are converted from monovalent (Ag+) to zerovalent (Ag0) state by the presence of phenols, carbohydrates, and terpenoids which are biomolecules that act as stabilizing and capping agents (Thivaharan, Ramesh and Raja, 2018).

In this study, the leaf extracts of Hibiscus rosa-sinensis (red, vermillion, pink, orange, yellow and pokuru wada) were used to synthesize AgNPs. Previous studies have proved that these leaves possess strong antibacterial, and antioxidant properties (Ngan et al., 2021). Hibiscus rosa-sinensis is a tropical Asian plant that belongs to the family Malvacae. The flowers, as well as the leaves, have medicinal properties which consist of, anti-aging and anti-depressant and antioxidant properties, help in improving digestion and losing weight, lowering cholesterol and blood pressure, menstruation, stimulation of blood circulation, and in preventing cancer (Lybrate, 2020).

An appropriate equilibrium between free radical generation and antioxidant

defenses is fundamental to life. Free radicals are a molecular species capable of independent existence even though they have unpaired electrons in the valence electron shell whereas antioxidants neutralize free radicals by giving up their own electrons (Figure 2) (Lobo et al., 2010).

Antioxidants can be divided into two primary categories: natural and synthetic. Recent research has revealed that synthetic antioxidants may have harmful side effects, expensive, and show less efficacy than natural antioxidants. Interest in consuming natural antioxidants has significantly expanded for these reasons, particularly in developed countries, due to its greater affordability, higher antioxidant activity, and impacts on longevity. Hence, they have been the subject of several studies for a long time and are still utilized in many different areas for a variety of purposes (Zehiroglu and Sarikaya, 2019).

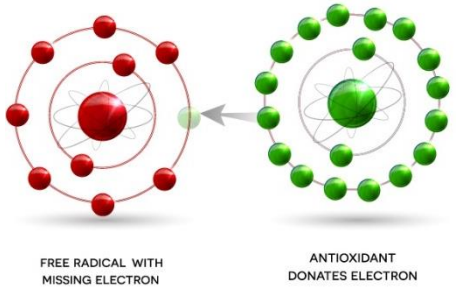

Figure 2: Antioxidants and free radicals (McCann, 2020)

Oxidative stress (OS) is a physiological phenomenon that arises due to the increase in oxidant processes as a result of the lack of antioxidant defense in the body. OS has the potential to harm a wide range of molecule species (proteins, lipids, fatty acids, DNA). Upregulation of OS has been linked to diseases such as cancer, atherosclerosis, cardiovascular disease, neurological and endocrinological problems, and diabetes, which are caused by an excess of reactive oxygen species (ROS) or a diminished scavenging contribution (Calvani, Pasha and Favre, 2020).

Based on previous studies, Hibiscus rosa-sinensis leaves have been considered as a good source of antimicrobial properties. All parts of the plant could be utilized for pharmacological purposes due to their effectiveness and safety. The extracts of Hibiscus rosa-sinensis leaves have immense potential to be used in treating infections caused by S. aureus. In addition, S. typhimurium, E. coli and P. aeruginosa have shown 100 % sensitivity to the leaf extracts (Uddin et al., 2010).

Photocatalytic degradation of dyes and other organic pollutants has been a focus of research since the twentieth century. Direct discharge of numerous organic pollutants, particularly azo dyes, which are widely employed in various products, including clothing, furniture, plastics, textile, food, and paper sectors, causes significant damage to the ecosystem (Viswanathan, 2018). Due to the poisonous, mutagenic, and carcinogenic properties of azo dyes and their transformation products, their unregulated release into the environment is concerning. Flocculation adsorption, ion exchange, UV radiation, ozonization, and photochemical processes of electrochemical destruction can be used to remove these dyes (Sharma et al., 2015). However, due to its low cost, abundance, high oxidative properties, high photostability, and simple, rapid, and effective mechanism of degradation, AgNPs have recently gained attention as photocatalysts for the degradation of poisonous dyes such as Methylene Blue, Methyl Orange, Rhodamine B, and Methyl Red (Figure 3) (Shaikh et al., 2021).

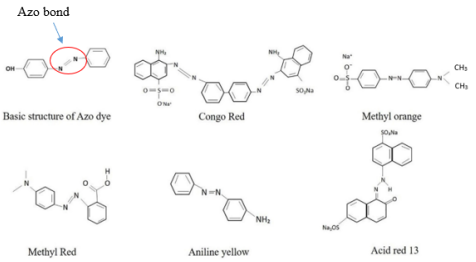

Figure 3: *Structure of the common dyes containing azo bonds (Mishra et al., 2022)*

This project aims to synthesize eco-friendly AgNPs using six varieties of Hibiscus rosa-sinensis leaves to assess their antioxidant, antibacterial, and photocatalytic properties. The antioxidant activity is determined by Total Flavonoid Content (TFC), Total Phenolic Content (TPC), and Total Antioxidant Content (TAC). The well diffusion technique was performed to determine antimicrobial activity using Escherichia coli and Staphylococcus aureus. Photocatalytic activity of AgNPs was assessed by using commercially available Methyl Orange dye. Hence, by achieving these objectives AgNPs can be a valuable technique to recycle leaves to treat free radical-induced illnesses and create a better environment free of harmful azo dyes.

MATERIALS AND METHODOLOGY

Materials

Chemicals and Reagents: Silver nitrate (AgNO3), Molisch's reagent, concentrated sulfuric acid (H2SO4), 3% Ferric Chloride (FeCl3), Millon's reagent, Ninhydrin solution, Wagner's reagent, ammonia solution, sodium hydroxide (NaOH), aluminium chloride (AlCl3), potassium acetate (CH3COOK), Folin-Ciocalteu phenol reagent, sodium carbonate (Na2CO3), sodium sulfate (Na2SO4), ammonium molybdate ([NH4]6 Mo7O24.4H2O), chloroform (CH3Cl), methylene orange dye (C14H14N3NaO3S), sodium borohydride (NaBH4), and Muller-Hinton's Agar, methanol, 2-diphenyl-1-picrylhydrazyl (DPPH), Gentamycin, saline

Instrumentation: Electronic balance, hot air oven, spectrophotometer, water bath, incubator, refrigerator, fume hood, and autoclave.

Glassware & Consumables: Aluminum foil, Whatmann No.1 filter paper, falcon tubes, clamps, funnel, beakers, glass rod, gloves, permanent marker, measuring cylinder, test tubes, test tube racks, cuvettes, tissues, micropipettes, Pasteur pipettes, micropipette tips, watch glass, spatulas, watch glass, conical flask, petri plates.

METHODOLOGY

Prior to conducting the research COOSH forms were filled for safety purposes. COOSH assessment focuses on dangers and risks posed by hazardous substances in the laboratory.

Sample collection:

Six varieties of Hibiscus rosa-sinensis leaves; red, vermillion, pink, orange, yellow, and pokuru wada, were collected from Derani Plants Nursery, Piliyandala (Figure 4).

Figure 4: Six varieties of Hibiscus rosa-sinensis

Sample Preparation using Distilled Water:

The fresh leaves were collected and cleaned to remove dust and other impurities. Afterwards, the leaves were dried using the hot-air oven. 2g of each variety was mixed with 50mL of distilled water before being incubated for 20

minutes at 60℃. The extract was filtered through Whatmann No.01 filter paper into 50mL falcon tubes and stored at 4℃ in the refrigerator until further use.

Phytochemical Analysis

The aqueous extracts of all six varieties of Hibiscus leaves were tested for the following phytochemicals using standard procedures (Table 1).

Green Synthesis of Silver Nanoparticles

Phytochemical tests	Methodology	Results
Carbohydrates	0.5mL of plant leaf extract was mixed with 250µL of Molisch's reagent and few drops of concentrated H_2SO_4 acid.	Formation of a purple colour ring.
Amino acids	1 drop of Ninhydrin solution was added to 0.5mL of plant extract and heated in a boiling water bath.	Appearance of a purple colour.
Saponins	1mL of distilled water was added to 0.5mL of each plant extract and shaken vigorously in a test tube for 2 minutes.	Formation of a 1cm layer of foam.
Proteins	To 0.5mL of plant extract, few drops of Millon's reagent was added.	Formation of a white precipitate.
Quinones	To 0.5mL of leaf extract, 0.5mL of conc. H_2SO_4 acid was added along the wall.	Formation of red colour.
Anthraquinones	0.5mL of plant extract was mixed with chloroform and 0.5mL of ammonia solution was added	Presence of pink, red, violet colour.
Tannins	1mL of 3% $FeCl_3$ was added to 0.5mL of each leaf extract.	Formation of greenish black.
Terpenoids	0.5mL of plant leaf extract was mixed with 0.75mL and few drops of conc. H_2SO_4 was added along the wall.	Formation of a reddish-brown interface.

1mL of each extract was added to 9mL of 1mM AgNO3 and was incubated for 1 hour at 90℃. Using distilled water as a blank, the absorbance was measured using a UV-Spectrophotometer from 320nm to 500nm (Abhayawardena and Kandiah, 2020).

SEM Analysis

3mL of Yellow AgNP sample was transferred into an Eppendorf tube and was centrifuged at 13500rpm for 10 seconds, multiple times. The sample was then dried completely at 50℃ overnight and was sent to SLINTECH, Homagama for SEM analysis. Hitachi SU6600 SEM was used to generate images.

Dilution of samples

1mL of each leaf extract and AgNPs were obtained and diluted with 14mL distilled water resulting in 1:15 dilution. Following the dilution, the samples underwent the following assays in triplicates.

Determination of the Total Flavonoid Content (TFC)

TFC was determined by the Aluminum Chloride method. The reaction mixture comprised of 1mL of extract, 0.5mL of $AlCl_3$ (1.2%) and 0.5mL of 120mM potassium acetate. After incubating the mixture for 30 minutes at room temperature (RT), the absorbance was measured at 415nm using a blank of distilled water. The concentration was expressed in Quercetin equivalence (mg QE/ 100g) (Garg *et al*., 2012).

Determination of the Total Phenolic Content (TPC)

TPC was determined by Folin-Ciocalteu reagent method. 1mL of the extract was added with 0.1mL of Folin-Ciocalteu reagent (1:4 dilution) followed by incubation for 15 minutes at RT. 2.5mL of saturated sodium carbonate was added and incubated at RT for 30 minutes. The absorbance was measured at 760nm with a blank of distilled water. The concentration was expressed in Gallic acid equivalence (g GAE/ 100g) (Garg *et al*., 2012).

Determination of the Total Antioxidant Content (TAC)

TAC was determined by mixing 1mL of prepared solution (0.6M sulfuric acid, 28mM sodium sulfate and 4mM ammonium molybdate in 1:1:1 ratio) with diluted sample 3mL and incubated for 90 minutes at 90℃. Following incubation, distilled water was used as a blank to measure the absorbance at 695nm. The concentration was expressed in Ascorbic acid equivalence (mg AAE/ 100g) (Perera and Kandiah, 2018).

Determination of 2, 2-Diphenyl-1-picrylhydrazyl (DPPH) Scavenging Activity

0.004g of DPPH was dissolved in 100mL of methanol. 2mL of DPPH solution was mixed with 1mL of the diluted (1:15) sample and was incubated in dark, for 30 minutes at RT. Methanol was used as blank and the absorbance was measured at 517nm. Using the following equation (1), the percentage DPPH scavenging activity was calculated:

$$\text{DPPH activity (\%)} = \frac{\text{A control} - \text{A sample}}{\text{A control}} \times 10 \quad (1)$$

Median Inhibitory Concentration (IC50)

2mL of DPPH solution was mixed with diluted samples and distilled water in a series of five concentrations, consisting of 100%, 80%, 60%, 40%, and 20%. Using methanol as a blank, the absorbance of each sample was measured at 517nm. Equation (1) was used to calculate the percentage DPPH scavenging activity.

Determination of the Photocatalytic activity

UV light

The yellow AgNP sample was selected to assess the photocatalytic activity. 0.5mL of 4000ppm sample was added into 50mL of 1mM methyl orange solution. It was kept under UV light and the absorbance was measured from 300nm to

580nm every 10 minutes up to 80 minutes. The same procedure was followed for the 267ppm yellow AgNP sample as well, and the absorbance was measured for 120 minutes.

Sun light

0.5mL of 4000ppm yellow AgNP sample was added into 50mL of 1mM methyl orange solution. It was kept under the sunlight and the absorbance was measured from 300nm to 580nm every 10 minutes up to 200 minutes. The same procedure was followed for the 267ppm yellow AgNP sample as well, and the absorbance was measured for 160 minutes.

With the NaBH4 catalyst

4000ppm yellow AgNP sample and 0.5mL of 0.2M NaBH4 were added into 50mL of 1mM Methyl Orange. The absorbance was measured from 300nm to 580nm using distilled water as a blank every 10 minutes for 90 minutes. The same procedure was repeated for 267ppm yellow sample and was measured for 60 minutes (Kandiah and Chandrasekaran, 2021).

Determination of the Antimicrobial Activity

Muller Hinton's agar was boiled and autoclaved for 15 minutes and it was poured into sterilized petri dishes and they were left to solidify. This procedure was carried out in an aseptic environment. Afterwards, the bacterial culture of E. coli and S. aureus was uniformly spread on the plates using a cotton swab. As illustrated in figure 5, the petri plates were separated into four quadrants and three wells were made on the agar plates for the duplicates of the sample (S1 and S2) and the negative control. 1mL of saline was loaded into the negative control, whereas 100µl of the sample was loaded into S1 and S2 each. Gentamycin discs were utilized as the positive control. Following this, the petri dishes were incubated overnight at 37℃. Using a ruler the zone of inhibition (ZOI) was measured.

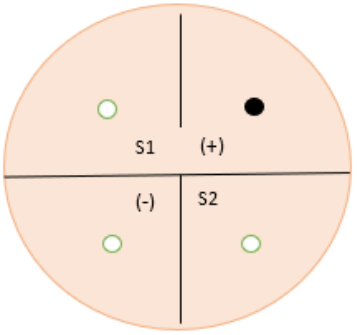

Figure 5: *Illustration of the petri plate wells*

Statistical Analysis

Using the software Microsoft Excel 2019 version, one-way ANOVA tables were generated and the correlation between antioxidant assays was assessed using the statistical software SPSS.

RESULTS

Phytochemical Screening

Phytochemical	Carbohydrates	Amino Acids	Saponins	Proteins	Quinones	Anthraquinones	Tannins	Terpenoids
Red	✓	×	✓	✓	✓	×	✓	✓
Vermillion	✓	✓	✓	✓	✓	×	✓	✓
Pink	✓	✓	✓	✓	✓	×	✓	✓
Orange	✓	×	✓	✓	✓	×	✓	✓
Yellow	✓	×	✓	✓	✓	×	✓	✓
Pohuni	✓	✓	✓	✓	✓	×	✓	✓
Results								

Table 2: Phytochemicals present in Hibiscus rosa-sinensis leaf extracts

Phytochemicals present in Hibiscus rosa-sinensis leaf extracts were analyzed using standard procedures.

Hibiscus rosa-sinensis leaf extracts consist all of the above-mentioned phytochemicals except anthraquinones. Red, orange and yellow leaf extracts did not show positive results for the presence of Amino acids.

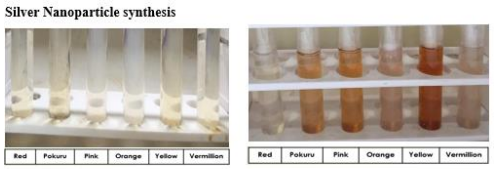

Figure 6: *Before (left) and after (right) AgNP synthesis (heated at 90°C for 60 minutes)*

The colourless water extracts of pokuru, pink, orange and yellow samples turned brown indicating the formation of silver nanoparticles. The optimization was observed at 90°C for 60 minutes and the absorbance was measured from 320nm to 500nm

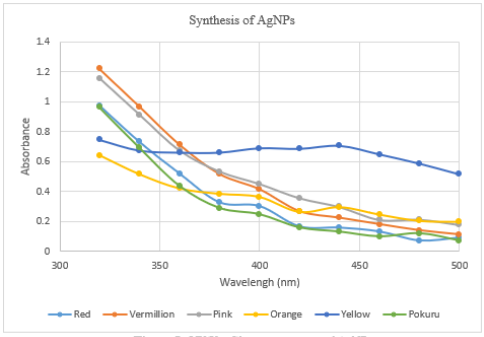

Figure 7: *UV/Vis Characterization of AgNPs*

The peak was observed from wavelengths 410nm to 480nm indicating the presence of AgNPs. The water extracts were heated at different temperatures for different time limits for optimization purposes.

Table 3: *Optimization table*

Sample Name	90°C				60°C				RT
	15 mins	30 mins	45 mins	60 mins	15 mins	30 mins	45 mins	60 mins	24 hours
Red	×	✓	×	×	×	×	×	×	×
Vermilion	×	×	×	×	×	✓	×	✓	✓
Pink	×	×	✓	✓	×	✓	×	×	×
Orange	✓	✓	×	✓	✓	×	✓	×	×
Yellow	✓	✓	✓	✓	×	✓	✓	×	✓
Pokuru wada	✓	✓	✓	✓	×	×	×	✓	✓

SEM Analysis

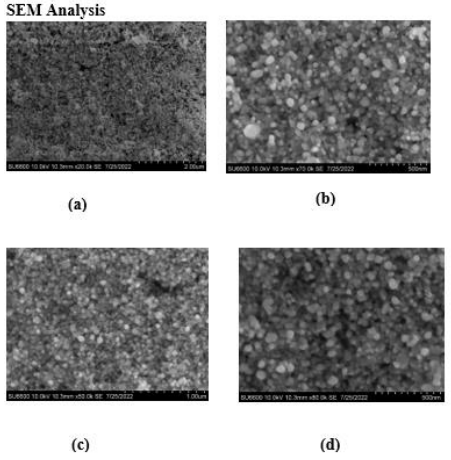

Figure 8: SEM Analysis of yellow AgNPs optimized at 90°C for 60 minutes

The yellow AgNPs were 50nm in size and spherical in shape.

Total Flavonoid Content (TFC)

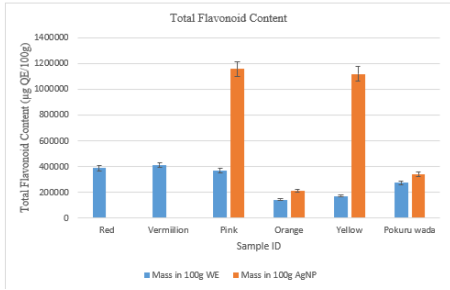

Figure 9: Total Flavonoid Content in Water Extracts and AgNPs

Higher TFC was shown in all nanoparticles, yellow and pink being the highest. The significant difference between water extracts and AgNPs was compared using one way-ANOVA. The P

value was obtained as 0.08 and there was no significant difference.

Anova: Single Factor						
SUMMARY						
Groups	*Count*	*Sum*	*Average*	*Variance*		
Column 1	6	1752604.167	292100.7	1.33E+10		
Column 2	4	2825520.834	706380.2	2.53E+11		
ANOVA						
Source of Variation	*SS*	*df*	*MS*	*F*	*P-value*	*F crit*
Between Groups	4.11906E+11	1	4.12E+11	3.992488	0.080751	5.317655
Within Groups	8.25362E+11	8	1.03E+11			
Total	1.23727E+12	9				

Table 4: *ONE-Way ANOVA for TPC in water extracts and AgNPs*

Total Phenolic Content (TPC)

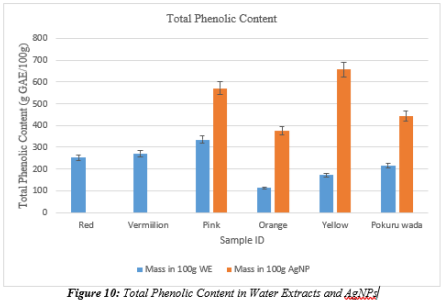

Figure 10: *Total Phenolic Content in Water Extracts and AgNPs*

All AgNPs showed higher TPC values than the water extracts. Significant difference between water extracts and AgNPs was compared using one way-ANOVA. A P value of 0.002 was obtained.

Table 5: One-Way ANOVA for TPC in water extracts and AgNPs

Anova: Single Factor

SUMMARY						
Groups	*Count*	*Sum*	*Average*	*Variance*		
Column 1	6	1358.571429	226.4286	6055.051		
Column 2	4	2046.428571	511.6071	16049.11		
ANOVA						
Source of variation	*SS*	*df*	*MS*	*F*	*P-value*	*F crit*
Between Groups	195184.3622	1	195184.4	19.91104	0.002105	5.317655
Within Groups	78422.57653	8	9802.822			
Total	273606.9388	9				

Total Antioxidant Content (TAC)

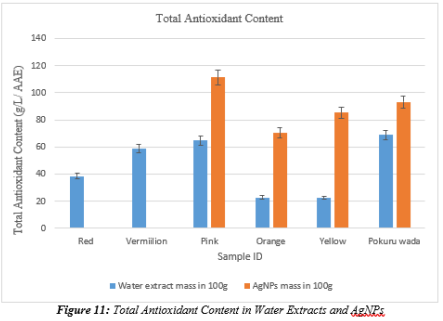

Figure 11: *Total Antioxidant Content in Water Extracts and AgNPs*

All AgNPs showed higher TAC whereas pink showed the highest TAC. Significant difference between water extracts and AgNPs was compared using one way-ANOVA. A P value of 0.008 was obtained.

Table 6: ONE-Way ANOVA for TAC in water extracts and AgNPs

Anova: Single Factor

SUMMARY						
Groups	*Count*	*Sum*	*Average*	*Variance*		
Column 1	6	276.1363636	46.02273	438.9101		
Column 2	4	360.2272727	90.05682	290.4399		
ANOVA						
Source of Variation	*SS*	*df*	*MS*	*F*	*P-value*	*F crit*
Between Groups	4653.602789	1	4653.603	12.14299	0.008263	5.317655
Within Groups	3065.870351	8	383.2338			
Total	7719.47314	9				

DPPH Radical Scavenging Assay

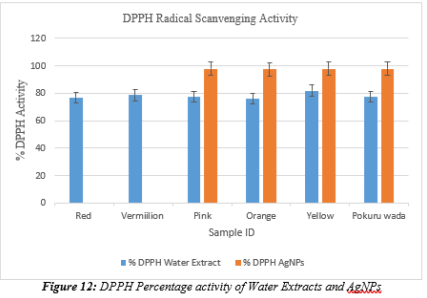

Figure 12: *DPPH Percentage activity of Water Extracts and AgNPs*

AgNPs showed a higher percentage of DPPH activity than the water extracts.

Inhibitory Concentration (IC50) of DPPH

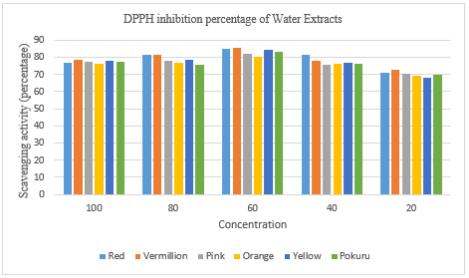

Figure 13: DPPH Percentage inhibition of water extract

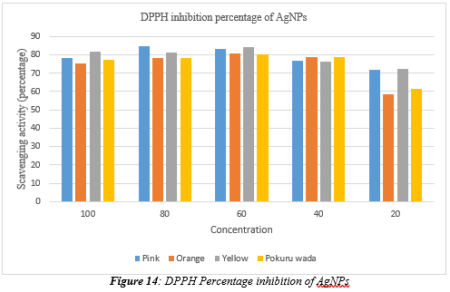

Figure 14: DPPH Percentage inhibition of AgNPs

Sample	Water Extract	AgNPs
Red	831.94	-
Vermillion	650.19	-
Pink	648.50	479.84
Orange	720.46	304.13
Yellow	470.36	406.83
Pokuru wada	698.32	317.46

***Table 2**: Inhibitory concentration (IC_{50}) of samples*

Lower IC_{50} values in AgNPs indicate higher antioxidant capacity.

Determination of Photocatalytic activity

UV Light

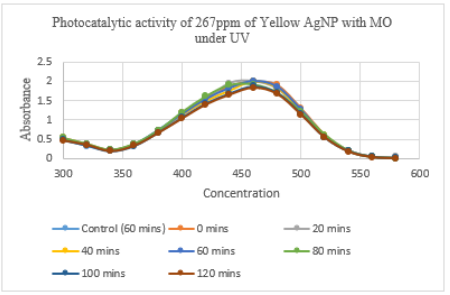

Figure 15: Photocatalytic activity of 267ppm of Yellow AgNPs under the UV light

There was no degradation of the 267ppm yellow AgNPs under UV.

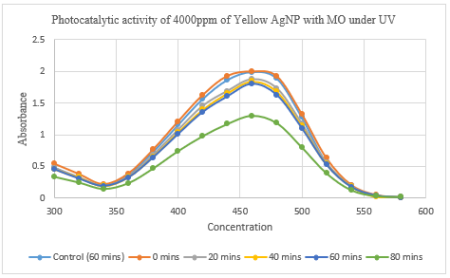

Figure 16: Photocatalytic activity of 4000ppm of Yellow AgNPs under the UV light

Under UV the 4000ppm yellow AgNPs did not start degrading until the 80th minute.

Sun Light

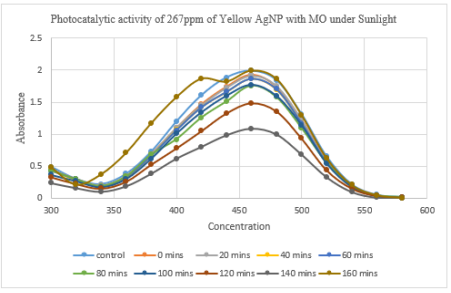

Figure 17: Photocatalytic activity of 267ppm of Yellow AgNPs under sun light

267ppm yellow AgNPs started degrading at 120 minutes.

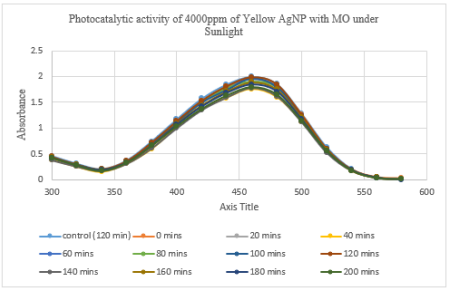

Figure 18: Photocatalytic activity of 4000ppm of Yellow AgNPs under sun light

There was no degradation observed in 4000ppm yellow AgNPs under UV.

With NaBH4 catalyst

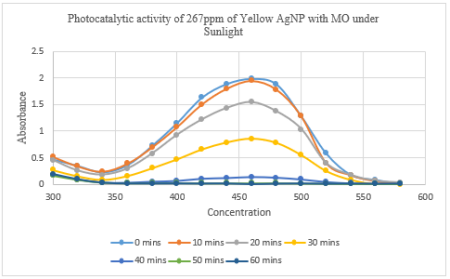

Figure 19: Photocatalytic activity of 267ppm of Yellow AgNPs with NaBH4

The photocatalytic degradation of Methyl Orange by 267ppm yellow AgNPs has been completely degraded within 60 minutes.

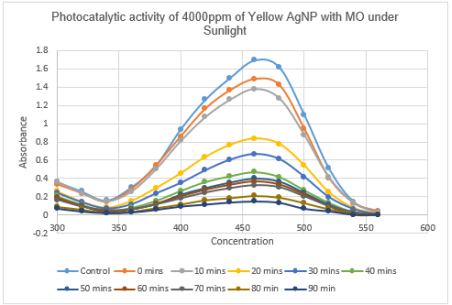

Figure 20: Photocatalytic activity of 4000ppm of Yellow AgNPs with NaBH4

The photocatalytic degradation of Methyl Orange by 4000ppm yellow AgNPs has been completely degraded within 90 minutes.

The orange colour became colourless within a few minutes as depicted below

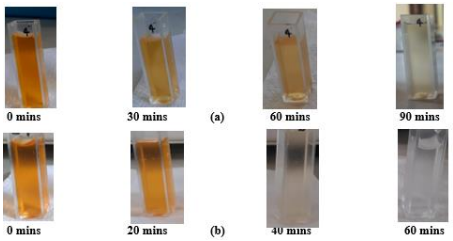

Figure 21: Decolourization of Methyl orange (a) 4000ppm AgNP sample (b) 267ppm AgNP sample

Antibacterial Activity

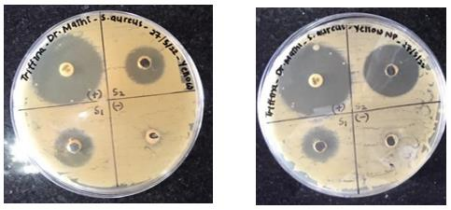

Figure 22: ZOI of S. aureus in yellow water extract (left) and yellow AgNPs (right)

The ZOI of S. aureus in yellow AgNPs was higher than its water extract. Significant difference between water extracts and AgNPs was compared using one way-ANOVA. A P value of 0.014 was obtained.

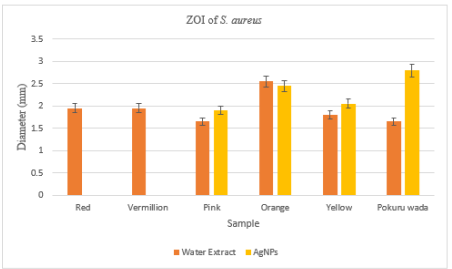

Figure 23: *ZOI of S. aureus water extracts and AgNPs*

Anova: Single Factor

SUMMARY						
Groups	*Count*	*Sum*	*Average*	*Variance*		
Column 1	6	11.55	1.925	0.11175		
Column 2	4	9.2	2.3	0.165		
ANOVA						
Source of Variation	*SS*	*df*	*MS*	*F*	*P-value*	*F crit*
Between Groups	0.3375	1	0.3375	2.562278	0.148108	5.317655
Within Groups	1.05375	8	0.13171875			
Total	1.39125	9				

Table 8: ONE-Way ANOVA for ZOI of water extracts and AgNPs for S. aureus

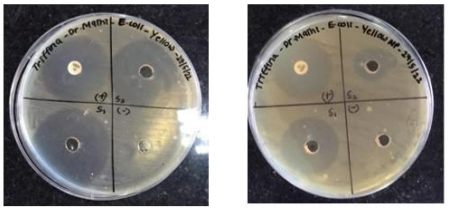

Figure 24: *ZOI of E. coli in yellow water extract (left) and yellow AgNPs (right)*

The ZOI of E. coli in Yellow AgNPs was lower than its water extract. However, pink and orange nanoparticles showed a higher ZOI of E. coli. Significant difference between water extracts and AgNPs was compared using one way-ANOVA. A P value of 0.89 was obtained

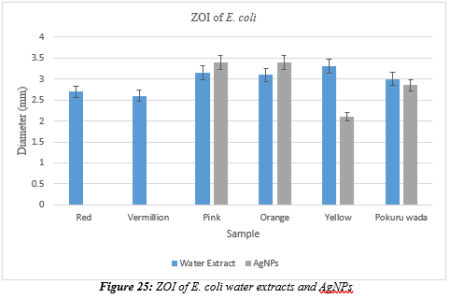

Figure 25: *ZOI of E. coli water extracts and AgNPs*

Table 9: ONE-Way ANOVA for ZOI of water extracts and AgNPs for E. coli

Anova: Single Factor

SUMMARY						
Groups	*Count*	*Sum*	*Average*	*Variance*		
Column 1	6	17.85	2.975	0.07375		
Column 2	4	11.75	2.9375	0.378958		
ANOVA						
Source of Variation	*SS*	*df*	*MS*	*F*	*P-value*	*F crit*
Between Groups	0.003375	1	0.003375	0.017933	0.896779	5.317655
Within Groups	1.505625	8	0.188203125			
Total	1.509	9				

Table 10: ONE-Way ANOVA for ZOI of water extracts and AgNPs for E. coli and S. aureus

Anova: Single Factor

SUMMARY						
Groups	*Count*	*Sum*	*Average*	*Variance*		
Column 1	10	20.75	2.075	0.154583		
Column 2	10	29.6	2.96	0.167667		
ANOVA						
Source of Variation	*SS*	*df*	*MS*	*F*	*P-value*	*F crit*
Between Groups	3.916125	1	3.916125	24.30489	0.000108	4.413873
Within Groups	2.90025	18	0.161125			
Total	6.816375	19				

The generated ONE-Way ANOVA showed a significant difference between S. aureus and E. coli with a P value of 0.0001.

DISCUSSION

In recent years, green synthesis of metallic nanoparticles has emerged as a new promising field of study (Malhotra and Alghuthaymi, 2022). "Green synthesis of nanomaterials" describes the production of various metal nanoparticles using numerous bioactive substances. Researchers are investigating the use of microbes, plant extracts, and other biomaterials in response to the growing demand to produce "green" and affordable production processes for metal nanoparticles (Zhu, Pathakoti and Hwang, 2019). The goal of green synthesis of nanoparticles is to reduce waste production and use eco-friendly methods. The likelihood of environmental pollution is significantly decreased when natural bioactive agents are used in the manufacture of metal nanoparticles (Dhand, Kumari and Padma, 2021).

The link between nanomaterials and antibacterial activity is that, "nanomaterials as antibacterial complements to antibiotics are highly promising and generate significant interest as they might bridge the gaps where medicines commonly fail" (Wang, Hu and Shao, 2017). The non-specific bacterial toxicity mechanisms of metal-based nanoparticles not only make it challenging

for bacteria to acquire resistance, but also widen the range of antibacterial activity (López et al., 2020). Due to the capacity to fine-tune their properties and enable highly specialized photocatalysis, nanomaterials are significant in photocatalytic research (Li, 2020).

Water is the most polar solvent used in the extraction of plant extract. It is also inexpensive, harmless, and dissolves a variety of compounds compared to other compounds such as alcohol, chloroform, ether etc. The heat was utilized throughout the extraction process to accelerate the extraction, reduce the viscosity of the solvent and enhance the removal of secondary metabolites such as flavonoids, phenols, terpenoids etc. (Abubakar and Haque, 2020). The current study conducted green synthesis of AgNPs. Silver was particularly utilized as it possesses distinctive properties which include high electrical conductivity, optical, electrical, thermal, and biological characteristics. Interestingly, biologically synthesized AgNPs exhibit great yield, solubility, and stability (Zhang et al., 2016). Moreover, due to their antibacterial activity against a range of pathogens, AgNPs have lately gained recognition as potential materials in the biomedical sciences (Koduru et al., 2018).

Phytochemical screening confirmed the presence of phenols, saponins, flavonoids, terpenoids, tannins, quinones, and proteins for Hibiscus rosa-sinensis. These phytochemicals were used in the green synthesis of AgNPs as a capping and a stabilizing agent (Dada et al., 2019). As a result of synthesizing AgNPs, four samples out of six showed a colour change from colourless to brown with distinct peaks between the range of 400nm to 480nm indicating the formation of AgNPs due to the Surface Plasmon Resonance phenomena; a consequence of the collective oscillations of free electrons on the surface of metallic particles (Ider et al., 2016).

SEM analysis was performed to describe the morphology and characterization of AgNPs. It was observed that the yellow AgNPs were 40-50nm in size and spherical. Similar studies have shown the spherical shape of the Hibiscus rosa-sinensis leaves AgNPs with a particle size of 48.5nm (Lu et al., 2022). The optical properties of the synthesized AgNPs were analyzed using UV-Visible absorbance spectroscopy. The energy difference between the top of the valence band (VB) and the bottom of the conduction band (CB) is referred to as the "band gap". It has the ability to leap from one band to the next and is used to examine the conductivity of the produced nanomaterials. It takes a certain minimum amount of energy, known as band energy, for an electron to shift from a VB to a CB. The materials can be divided into semiconductors (<3eV) and insulators (>4eV) based on the band gap energies (Sundeep et al., 2017).

Using Planck's equation (2), the band gap energies of synthesized AgNPs were calculated.

$$E = h C/\lambda \qquad (2)$$

E = Band gap energy; h = Planck's constant (6.6269×10^{-34}Js)

C = Speed of light; λ = Maximum absorption wavelength for each

Sample	Band gap energy	Classification
Pink	2.58	Semiconductor
Orange	2.82	Semiconductor
Yellow	2.82	Semiconductor
Pokuru wada	2.58	Semiconductor

Table 3: *Conductivity classification of synthesized AgNPs*

As the bandgap energies of all samples were <3eV, the AgNPs were classified as semiconductors (Table 11).

The antioxidant content of water extracts and synthesized AgNPs was

evaluated using the following antioxidant assays and the results obtained can be correlated with previously carried out studies.

TFC was determined using the aluminum chloride (AlCl3) method. TFC was estimated by an acid stable complex formed between the AlCl3 and the keto-groups of C-4 atoms and the adjacent hydroxyl groups at C-3 or C-5 atoms, with a maximum absorption being 415nm. In addition, acid labile complexes are produced with orthodihydroxyl groups in A- or B- ring of flavonoids (Figure 26). Quercetin, a flavanol with nearby hydroxyl groups at the C-3 and C-5 atoms and keto groups at the C-4 atoms, served as the standard control for determining the flavonoid concentration (Ilmi, Elya and Handayani, 2020).

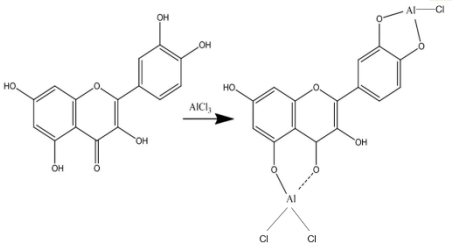

Figure 26: Mechanism of the reaction in TFC (Ilmi, Elya and Handayani, 2020).

Overall, compared to the water extracts AgNPs contained higher TFC, pink AgNPs being the highest. TFC among AgNPs were pink>yellow>pokuru>orange and TFC among water extracts were red=vermillion>pink=pokuru>yellow=orange. The generated one-way ANOVA showed P>0.05, thereby demonstrating that there is no significant difference between water extracts and AgNPs. Weerasinghe and his co-workers observed the same in Hibiscus rosa-sinensis flower extracts in 2021.

The Total Phenol Content (TPC) relies on the principle of Folin-Ciocalteu (FC) reagent method. FC assay is based on the electrons transferring from phenolic substances to phosphotungstic or phosphomolybdic acid complexes under alkaline conditions (Figure 27). The transfer of electrons facilitates a change in colour from yellow to pale-blue by the phenolic compounds which can be detected at 760nm in the UV-visible spectrum. (Ford et al., 2019).

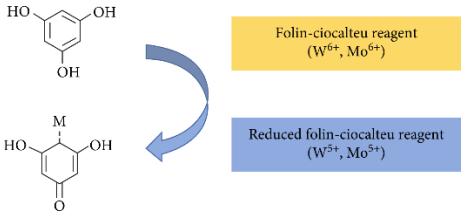

Figure 27: Mechanism of the reaction in TPC (Hernandez, Ocampo and Correa, 2021)

Compared to the water extracts, TPC in AgNPs was higher in the following manner: yellow>pink>pokuru>orange whereas TPC in water extracts were pink>vermillion=red=pokuru>yellow=orange. One-way ANOVA showed P<0.05, thereby demonstrating that there is a significant difference between AgNPs and water extracts. Nascimento and his associates (2021) discovered that Hibiscus rosa-sinensis flowers extracts represent a greater source of phenols with a significant difference of P=0.002 than the leaves.

TAC was assessed using the phosphomolybdenum method which reduces Mo (VI) to Mo (V) by antioxidant compounds followed by the formation of a Mo (V)/ green phosphate complex at acidic pH that can be detected at 695nm (Figure 28) (Fowsiya and Madumitha, 2017).

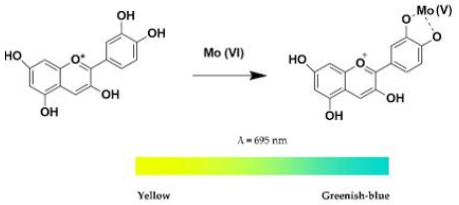

Figure 28: Mechanism of the reaction in TAC (Fowsiya and Madhumitha, 2017)

TAC content was higher in AgNPs than in the water extracts as follows: pink> yellow=pokuru> orange whereas, TAC in water extracts were as follows: pokuru=pink=vermillion>red>orange=yellow. As per the one-way ANOVA table which was generated, there was a significant difference ($P<0.05$) between the AgNPs and the water extracts. Gamage and his colleagues reported a significantly higher antioxidant content in Hibiscus rosa-sinensis leaves in 2021.

The DPPH test uses DPPH, a stabilized free radical with a single unpaired electron that is delocalized throughout the whole molecule. Based on the antioxidants' ability to donate electrons to the nitrogen in DPPH, the DPPH radical scavenging activity is assessed. DPPH possesses a purple color which turns to pale yellow as a result of the odd electron in the nitrogen pairs up (Figure 29). The decrease in DPPH absorption is proportional to the concentration of radicals being scavenged (Lian and Kitts, 2014; Lu et al., 2022).

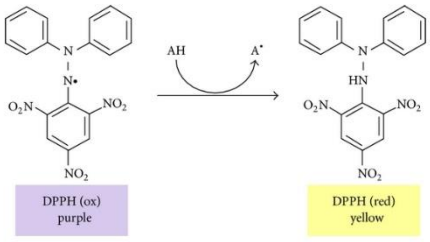

Figure 29: Principle of DPPH Assay (Teixeira et al., 2013)

Overall, the quenching ability of AgNPs was higher than the water extracts which correlates with higher TAC. DPPH percentage activity among AgNPs and water extracts were in the following manner: pink=yellow=pokuru=orange and yellow=vermillion=red=pink=pokuru>orange respectively. Similar studies conducted by Mak and his associates reported higher DPPH percentage activity observed in the Hibiscus rosa-sinensis flower extract in 2013.

IC50 or half maximal inhibitory concentration of a compound is the amount of antioxidants required to reduce the concentration of DPPH by 50%. According to studies, plant extracts with lower IC50 values have higher antioxidant action (Hadirah et al., 2021). According to table 7, AgNPs indicated lower IC50 values than water extracts demonstrating higher antioxidant activity in AgNPs. Orange AgNPs were found to have the lowest IC50 value compared to others, indicating the highest antioxidant capacity further correlating with its higher levels of TAC and TPC. Patel and his co-workers reported similar results in research conducted in 2012.

Pearson Correlation Coefficient (PCC) was performed on TFC, TPC, TAC assays and the statistical correlations between TPC and TAC and TFC and TPC were above 0.8 indicating a strong positive statistical correlation whereas, the correlation between TAC-TFC was moderate positive with a PCC of 0.698 (Figure 30). Thus, proving that both TFC and TPC contribute to TAC.

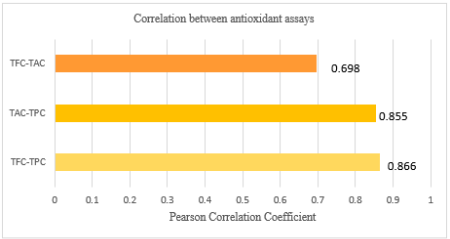

Figure 30: *Statistical correlation between antioxidant assays*

In photocatalysis, dye effluent treatment is a key mechanism whereby the electrons are excited from the VB to the CB upon irradiation resulting in the production of electron-hole pairs (Marimuthu et al., 2020). The dye is getting degraded by the generation of the electron and the hole in the VB and CB is caused by the excitation of the electron from the VB to CB. This excitation is a result of the surface plasmon resonance effect. Oxidative species; OH radicals are formed when the electrons transferred in the CB interact with H2O2 molecules. Additionally, when photo-induced holes in VB accept electrons from the OH- forming OH radicals, they attack the azo bond in the MO dye and cause degradation ultimately mineralizing the dye to a colorless product (Figure 31). NaBH4 provides AgNPs with additional electrons to form more radicals to result in rapid degradation of organic dyes (Naikwade et al., 2020; Latha et al., 2017).

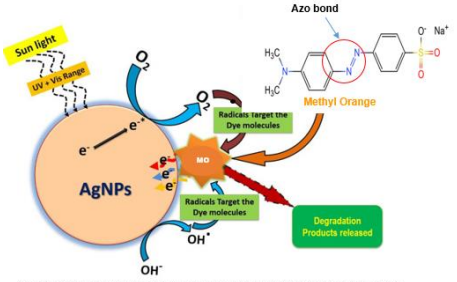

Figure 31: Photocatalytic activity of Silver Nanoparticles (Marimuthu et al., 2020)

In the current study photocatalytic activity was assessed using yellow AgNPs in the degradation of MO dye. The photocatalysis was assessed under UV, sunlight and under sunlight with NaBH4 catalyst. Under UV, 267ppm AgNPs did not show any degradation whereas the 4000ppm AgNPs started the degradation at 80 minutes. Under sunlight 267ppm AgNPs started the degradation at 120 minutes whereas 4000ppm did not show any degradation. AgNP samples 267ppm and 4000ppm completed the MO degradation within 60 minutes and 90 minutes respectively with the aid of NaBH4 catalyst under sunlight. The distinctive absorption peak of MO was found to be at 460nm.

The rate constant of the photocatalytic degradation was calculated using the following equation (3):

$$ln \frac{C}{Co} = -kt \qquad (3)$$

C = Methyl Orange Concentration	k = Rate constant
C_o = Initial Methyl Orange Concentration	t = Time

A higher rate constant (k) of 0.1048 was observed in 267ppm yellow AgNP sample than in 4000ppm sample (k = 0.0245). Thus, indicating that the photodegradation efficiency of 267ppm yellow AgNPs was relatively higher than 4000ppm yellow AgNPs (Figures 32 and 33). However, a catalytic study of MO with Derris trifoliate AgNPs showed a higher rate constant when the concentration of the AgNPs is higher (Cyril et al., 2019).

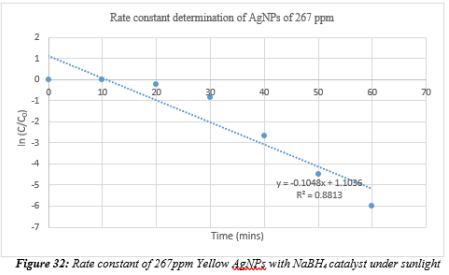

Figure 32: Rate constant of 267ppm Yellow AgNPs with $NaBH_4$ catalyst under sunlight

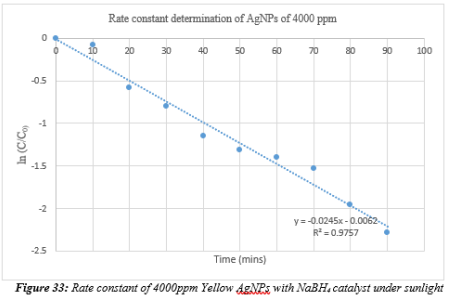

Figure 33: Rate constant of 4000ppm Yellow AgNPs with $NaBH_4$ catalyst under sunlight

The rate constant values under UV and sun light are as follows (Table 12):

Table 12: Rate constant values under UV and Sun light

Method	Sample	K Value
Sunlight	267ppm yellow AgNPs	0.0033
UV light	4000ppm yellow AgNPs	0.0045
$NaBH_4$ - Sunlight	267ppm yellow AgNPs	0.1048
$NaBH_4$ - Sunlight	4000ppm yellow AgNPs	0.0245

Parts of Hibiscus rosa-sinensis plant and the synthesized AgNPs consists of well-known for their antibacterial properties. The AgNPs have a propensity to penetrate through the microorganism cell walls and render the cell membrane inactive leading to cell death. The large surface area of AgNPs aids them in easily piercing through the cell membrane and interfering with the DNA replication of the microorganisms. The binding of silver ions with the DNA molecules inhibits the cells' ability to replicate and thus preventing the microorganism from proliferating. Hence the growth of the microorganisms is halted. Furthermore, AgNPs destroy the bacteria by producing ROS (Periasamy et al., 2022; Khanal et al., 2022). Antimicrobial activity tests indicated an increased antimicrobial activity against S. aureus in yellow AgNPs than in water extract. However, yellow water extracts showed higher antimicrobial activity against E. coli than AgNPs. Musimun and his colleagues (2022) reported that the decreased zone of inhibition could be due to the diluted concentration of AgNPs since previous studies have shown remarkable results for the antibacterial activity of Hibiscus rosa-sinensis AgNPs (Surya, Kumar and Rajakumar, 2016). Both generated One-way ANOVA tables didn't give any significant difference as the P value was greater than 0.05, but there was a significant difference between E. coli and S. aureus combined (Table 10).

In conclusion, four out of six samples produced AgNPs and all of them were semiconductors. SEM analysis images on yellow AgNPs depicted 50nm spherical-shaped AgNPs. The synthesized AgNPs exhibited higher antioxidant activity compared to the water extract. Photocatalytic degradation with NaBH4 catalyst was completed in both 267ppm and 4000ppm yellow AgNPs within 60 and 90 minutes respectively. Higher antimicrobial activity was shown against S. aureus in yellow AgNPs than in water extract. Thus, synthesizing AgNPs from Hibiscus rosa-sinensis may aid in producing various products for biological and medical applications.

Future work

- In the future, the same sample can be extracted using other solvents such as methanol. ethanol, chloroform, acetone and ether. Therefore, which solvent could extract polar active compounds and non-polar active compounds could be analyzed.
- Further antioxidant techniques including Ferric Reducing Ability of Plasma assay, total-peroxyl radical trapping parameter (TRAP), ABTS (2,2'-azino-bis-3-ethylbenzothiazoline-6-sulfonic acid) assay, Oxygen Radical Absorbance Capacity, can be performed to further analyze the antioxidant activity.
- High-resolution Transmission Electron Microscopic (TEM), dynamic light scattering (DLS), X-ray diffraction investigations can be used to observe and specify high resolution structures, morphology and dispersion of nanoparticles in order to further characterize the AgNPs.
- Apart from silver, green synthesis using other metals such as gold, copper, zinc, and cobalt nanoparticles could be synthesized in future.
- Hibiscus rosa-sinensis flower varieties can be collected from different parts of the country to conduct the antioxidant assays as the geographical area, environmental factors including

water, air, soil affects the antioxidant content in plant material.

- Photocatalytic degradation could be assessed using other synthetic dyes such as methyl red, methylene blue, malachite green, and Rhodamine B.
- Antibacterial activity of Hibiscus rosa-sinensis could be evaluated against other bacterial strains such as Pseudomonas aeruginosa and Bacillus subtilis in order to further determine their antimicrobial properties.
- Synthesized Hibiscus rosa-sinensis AgNPs could be further tested for wound healing and anticancer properties by using animal models. Thereby it could be used in future medical applications.
- Melamine adulteration is a fraudulent practice of increasing the protein content of food. Further evaluation could be done to detect the presence of melamine adulterant in milk using spectroscopic techniques.

REFERENCES

Abhayawardena, S. and Kandiah, M. (2020) 'Microwave Assisted Ecofriendly Silver Nanoparticle Synthesis Using Six Varieties of Capsicum Annuum: Evaluation Of Antioxidant, Antibacterial And Photocatalytic Properties', GARI International Journal of Multidisciplinary Research, 06(05), pp.48-60. [Online] Article ID: IN/GARI/ICHM/2020/167 (Accessed: 26 May 2022).

Abubakar, A. and Haque, M. (2020) 'Preparation of medicinal plants: Basic extraction and fractionation procedures for experimental purposes', Journal of Pharmacy and Bioallied Sciences, 12(1), p.1. [Online] DOI: 10.4103/jpbs.JPBS_175_19 (Accessed: 12 July 2022).

Calvani, M., Pasha, A. and Favre, C. (2020) 'Nutraceutical Boom in Cancer: Inside the Labyrinth of Reactive Oxygen Species', International Journal of Molecular Sciences, 21(6), p.1936. [Online] DOI: 10.3390/ijms21061936 (Accessed: 23 March 2022).

Carmona-Hernandez, J., Taborda-Ocampo, G. and González-Correa, C. (2021) 'Folin-Ciocalteu Reaction Alternatives for Higher Polyphenol Quantitation in Colombian Passion Fruits', International Journal of Food Science, 2021, pp.1-10. [Online] DOI: 10.1155/2021/8871301 (Accessed: 20 July 2022).

Cyril, N., George, J., Joseph, L. and Sylas, V. (2019) 'Catalytic Degradation of Methyl Orange and Selective Sensing of Mercury Ion in Aqueous Solutions Using Green Synthesized Silver Nanoparticles from the Seeds of Derris trifoliata', Journal of Cluster Science, 30(2), pp.459-468. [Online] DOI:10.1007/s10876-019-01508-9 (Accessed: 17 July 2022).

Dada, A., Adekola, F., Dada, F., Adelani-Akande, A., Bello, M., Okonkwo, C., Inyinbor, A., Oluyori, A., Olayanju, A., Ajanaku, K. and Adetunji, C. (2019) 'Silver nanoparticle synthesis by Acalypha wilkesiana extract: phytochemical screening, characterization, influence of operational parameters, and preliminary antibacterial testing', Heliyon, 5(10), p.e02517. [Online] DOI: 10.1016/j.heliyon.2019.e02517 (Accessed: 11 July 2022).

Dhand, V., Kumari, S. and Padma, P. (2021) 'Green synthesis of metallic nanoparticles: a review', Nanomaterials, pp.259-281. [Online] DOI: 10.1016/B978-0-12-822401-4.00022-2 (Accessed: 5 July 2022).

Fairuzi, A., Bonnia, N., Akhir, R., Akil, H., Yahya, S. and Rahman, N. (2018) 'Comparison studies on catalytic properties of silver nanoparticles biosynthesized via aqueous leaves extract of Hibiscus rosa-sinensis and Imperata cylindrical', AIP Conference Proceedings. [Online] DOI: 10.1063/1.5036858 (Accessed: 28 March 2022).

Gamage, D., Dharmadasa, R., Abeysinghe, D., Wijesekara, R., Prathapasinghe, G. and Someya, T. (2021) 'Assessment of Phytochemical Contents and Total Antioxidant Capacity of Five Medicinal Plants with Cosmetic Potential under Three Different Drying Methods', World Journal of Agricultural Research, 9(1), pp.24-28. [Online] DOI: 10.12691/wjar-9-1-4 (Accessed: 13 July 2022).

Garg, D., Shaikh, A., Muley, A. and Marar, T. (2012) 'In-vitro antioxidant activity and phytochemical analysis in extracts of Hibiscus rosa-sinensis stem and leaves', Free Radicals and Antioxidants, 2(3), pp.41-46. [Online] DOI:10.5530/ax.3.6 (Accessed: 26 May 2022).

Ider, M., Abderrafi, K., Eddahbi, A., Ouaskit, S. and Kassiba, A. (2016) 'Silver Metallic Nanoparticles with Surface Plasmon Resonance: Synthesis and Characterizations', Journal of Cluster Science, 28(3), pp.1051-1069. [Online] DOI: 10.1007/s10876-016-1080-1 (Accessed: 5 July 2022).

Ilmi, H., Elya, B. And HANDAYANI, R. (2020) 'Association Between Total Phenol and Flavonoid Contents in Artocarpus Heterophyllus (Jackfruit) Bark and Leaf Extracts and Lipoxygenase Inhibition', International Journal of Applied Pharmaceutics, pp.252-256. [Online] DOI: 10.22159/ijap.2020.v12s1.FF055 (Accessed: 17 March 2022).

Kandiah, M. and Chandrasekaran, K. (2021) 'Green Synthesis of Silver Nanoparticles Using Catharanthus roseus Flower Extracts and the Determination of Their Antioxidant, Antimicrobial, and Photocatalytic Activity', Journal of Nanotechnology, 2021, pp.1-18. [Online] DOI: https://doi.org/10.1155/2021/5512786 (Accessed: 26 March 2022).

Khanal, L., Sharma, K., Paudyal, H., Parajuli, K., Dahal, B., Ganga, G., Pokharel, Y. and Kalauni, S. (2022) 'Green Synthesis of Silver Nanoparticles from Root Extracts of Rubus ellipticus Sm. and Comparison of Antioxidant and Antibacterial Activity', Journal of Nanomaterials, 2022, pp.1-11. [Online] DOI: 10.1155/2022/1832587 (Accessed: 14 July 2022).

Koduru, J., Kailasa, S., Bhamore, J., Kim, K., Dutta, T. and Vellingiri, K. (2018) 'Phytochemical-assisted synthetic approaches for silver nanoparticles antimicrobial applications: A review', Advances in Colloid and Interface Science, 256, pp.326-339. [Online] DOI: 10.1016/j.cis.2018.03.001 (Accessed: 14 July 2022).

Latha, D., Arulvasu, C., Prabu, P. and Narayanan, V. (2017) 'Photocatalytic Activity of Biosynthesized Silver Nanoparticle from Leaf Extract of Justicia Adhatoda', Mechanics, Materials Science & Engineering, 9(1), pp.2412-5954. [Online] DOI: 10.2412/mmse.81.72.41 (Accessed: 16 July 2022).

Liang, N. and Kitts, D. (2014) 'Antioxidant Property of Coffee Components: Assessment of Methods that Define Mechanisms of Action', Molecules, 19(11), pp.19180-19208. [Online] DOI: 10.3390/molecules191119180 (Accessed: 21 July 2022).

Lobo, V., Patil, A., Phatak, A. and Chandra, N. (2010) 'Free radicals, antioxidants and functional foods: Impact on human health', Pharmacognosy Reviews, 4(8), p.118. [Online] DOI: 10.4103/0973-7847.70902 (Accessed: 25 March 2022).

Lu, L., Zhuang, Z., Fan, M., Liu, B., Yang, Y., Huang, J., Da, X., Mo, J., Li, Q. and Lu, H. (2022) 'Green formulation of Ag nanoparticles by Hibiscus rosa-sinensis: Introducing a navel chemotherapeutic drug for the treatment of liver cancer', Arabian Journal of Chemistry, 15(2), p.103602.[Online] DOI: 10.1016/j.arabjc.2021.103602 (Accessed: 21 July 2022).

Lybrate. (2020) Hibiscus Benefits and Its Side Effects [Online]. Available at:

<https://www.lybrate.com/topic/hibiscus-benefits-and-side-effects> (Accessed 23 March 2022).

Madkour, L. (2019) 'Introduction to Nanotechnology (NT) and Nanomaterials (NMs)', Advanced Structured Materials, pp.1-47. [Online] DOI: 10.1007/978-3-030-21621-4_1 (Accessed: 23 March 2022).

Mak, Y., Chuah, L., Ahmad, R. and Bhat, R. (2013) 'Antioxidant and antibacterial activities of hibiscus (Hibiscus rosa-sinensis L.) and Cassia (Senna bicapsularis L.) flower extracts', Journal of King Saud University - Science, 25(4), pp.275-282. [Online] DOI: 10.1016/j.jksus.2012.12.003 (Accessed: 14 July 2022).

Malhotra, S. and Alghuthaymi, M. (2022) 'Biomolecule-assisted biogenic synthesis of metallic nanoparticles', Agri-Waste and Microbes for Production of Sustainable Nanomaterials, pp.139-163. [Online] DOI: 10.1016/B978-0-12-823575-1.00011-1 (Accessed: 12 July 2022).

McCann, J. (2020) 'Free Radicals, Antioxidants and Disease', Empower Health Insurance [Online]. Available at: <https://empowerhealthinsuranceusa.com/free-radicals-antioxidants-and-disease/> (Accessed: 8 March 2022).

Mishra, A., Takkar, S., Joshi, N., Shukla, S., Shukla, K., Singh, A., Manikonda, A. and Varma, A. (2022) 'An Integrative Approach to Study Bacterial Enzymatic Degradation of Toxic Dyes', Frontiers in Microbiology, 12. [Online] DOI: 10.3389/fmicb.2021.802544 (Accessed: 12 July 2022).

Musimun, C., Papiernik, D., Permpoonpattana, P., Chumkaew, P. and Srisawat, T. (2022) 'Synergy of green-synthesized silver nanoparticles and Vatica diospyroides fruit extract in inhibiting Gram-positive bacteria by inducing membrane and intracellular disruption', Journal of Experimental Nanoscience, 17(1), pp.420-438. [Online] DOI: 10.1080/17458080.2022.2084533 (Accessed: 14 July 2022).

Naikwade, A., Jagadale, M., Kale, D., Gophane, A., Garadkar, K. and Rashinkar, G. (2020) 'Photocatalytic Degradation of Methyl Orange by Magnetically Retrievable Supported Ionic Liquid Phase Photocatalyst', ACS Omega, 5(1), pp.131-144. [Online] DOI: 10.1021/acsomega.9b02040 (Accessed: 16 July 2022).

Nasrollahzadeh, M., Sajadi, S., Sajjadi, M. and Issaabadi, Z. (2019) 'Applications of Nanotechnology in Daily Life', Interface Science and Technology, pp.113-143. [Online] DOI:10.1016/B978-0-12-813586-0.00004-3 (Accessed: 23 March 2022).

Ngan, L., Tan, M., Hoang, N., Thanh, D., Linh, N., Hoa, T., Nuong, N. and Hieu, T. (2021) 'Antibacterial activity of Hibiscus rosa-sinensis L. red flower against antibiotic-resistant strains of Helicobacter pylori and identification of the flower constituents', Brazilian Journal of Medical and Biological Research, 54(7). [Online] DOI: 10.1590/1414-431X2020e10889 (Accessed: 29 March 2022).

Patel, R., Patel, A., Desai, S. and Nagee, A. (2012) 'Study of Secondary Metabolites and Antioxidant Properties of Leaves, Stem and Root among Hibiscus Rosa-Sinensis cultivars', ASIAN J.EXP.BIOL.SCI, 3(4), pp.719-725. [Online] Available at: https://www.researchgate.net/publication/270479413_Study_of_Secondary_Metabolites_and_Antioxidant_Properties_of_Leaves_Stem_and_Root_among_Hibiscus_Rosa-Sinensis_cultivars (Accessed: 15 July 2022).

Paul, A., Karpagam, B. and Krishnaveni, N. (2016) 'Phytochemical Screening and antibacterial evaluation of the aqueous extracts of Hibiscus rosa-

sinensis' leaves against Aeromonas Hydrophila', International Journal of Advanced Science and Research, [Online]. Available at: https://www.researchgate.net/publication/326648387_Phytochemical_Screening_and_antibacterial_evaluation_of_the_aqueous_extracts_of_Hibiscus_rosa-sinensis'_leaves_against_Aeromonas_Hydrophila (Accessed: 27 May 2022).

Perera, B. and Kandiah, M. (2018) 'Microwave Assisted One-Pot Green Synthesis of Silver Nanoparticles Using Leaf Extracts from Vigna Unguiculate: Evaluation of Antioxidant and Antimicrobial Activities', International Journal of Multidisciplinary Studies, 5(2), p.62. [Online] DOI: 10.4038/ijms.v5i2.100 (Accessed: 26 May 2022).

Periasamy, S., Jegadeesan, U., Sundaramoorthi, K., Rajeswari, T., Tokala, V., Bhattacharya, S., Muthusamy, S., Sankoh, M. and Nellore, M. (2022) 'Comparative Analysis of Synthesis and Characterization of Silver Nanoparticles Extracted Using Leaf, Flower, and Bark of Hibiscus rosa-sinensis and Examine Its Antimicrobicidal Activity', Journal of Nanomaterials, 2022, pp.1-10. [Online] DOI: 10.1155/2022/8123854 (Accessed: 14 July 2022).

Sánchez-López, E., Gomes, D., Esteruelas, G., Bonilla, L., Lopez-Machado, A., Galindo, R., Cano, A., Espina, M., Ettcheto, M., Camins, A., Silva, A., Durazzo, A., Santini, A., Garcia, M. and Souto, E. (2020) 'Metal-Based Nanoparticles as Antimicrobial Agents: An Overview', Nanomaterials, 10(2), p.292. [Online] DOI: 10.3390/nano10020292 (Accessed: 10 July 2022).

Santos Nascimento, L., Gori, A., Raffaelli, A., Ferrini, F. and Brunetti, C. (2021) 'Phenolic Compounds from Leaves and Flowers of Hibiscus roseus: Potential Skin Cosmetic Applications of an Under-Investigated Species', Plants, 10(3), p.522. [Online] DOI: 10.3390/plants10030522 (Accessed: 13 July 2022).

Shaikh, W., Chakraborty, S., Owens, G. and Islam, R. (2021) 'review of the phytochemical mediated synthesis of AgNP (silver nanoparticle): the wonder particle of the past decade', Applied Nanoscience, 11(11), pp.2625-2660. [Online] DOI: 10.1007/s13204-021-02135-5 (Accessed: 24 March 2022).

Sharma, K., Singh, G., Singh, G., Kumar, M. and Bhalla, V. (2015) 'Silver nanoparticles: facile synthesis and their catalytic application for the degradation of dyes', RSC Advances, 5(33), pp.25781-25788. [Online] DOI:10.1039/c5ra02909k (Accessed: 29 March 2022).

Singh, J., Dutta, T., Kim, K., Rawat, M., Samddar, P. and Kumar, P. (2018) 'Green' synthesis of metals and their oxide nanoparticles: applications for environmental remediation', Journal of Nanobiotechnology, 16(1). [Online] DOI: 10.1186/s12951-018-0408-4 (Accessed: 24 March 2022).

Sundeep, D., Vijaya Kumar, T., Rao, P., Ravikumar, R. and Gopala Krishna, A. (2017) 'Green synthesis and characterization of Ag nanoparticles from Mangifera indica leaves for dental restoration and antibacterial applications', Progress in Biomaterials, 6(1-2), pp.57-66.[Online] DOI: 10.1007/s40204-017-0067-9 (Accessed: 14 July 2022).

Surya, S., Kumar, G. and Rajakumar, R. (2016) 'Green Synthesis of Silver Nanoparticles from Flower Extract of Hibiscus rosa-sinensis and Its Antibacterial Activity', International Journal of Innovative Research in Science, Engineering and Technology, 5(4), pp.5242-5247. [Online] DOI: 10.15680/IJIRSET.2016.0504129 (Accessed: 14 July 2022).

Teixeira, J., Gaspar, A., Garrido, E., Garrido, J. and Borges, F. (2013)

'Hydroxycinnamic Acid Antioxidants: An Electrochemical Overview', BioMed Research International, 2013, pp.1-11. [Online] DOI: 10.1155/2013/251754 (Accessed: 14 July 2022).

Thivaharan, V., Ramesh, V. and Raja, S. (2018) 'Green Synthesis of Silver Nanoparticles for Biomedical and Environmental Applications', Green Metal Nanoparticles, pp.287-439. [Online] DOI: 10.1002/9781119418900.ch12 (Accessed: 3 April 2022).

Uddin, B., Hossan, T., Paul, S., Ahmed, T., Nahar, T. and Ahmed, S. (2010) 'Antibacterial activity of the ethanol extracts of Hibiscus rosa-sinensis leaves and flowers against clinical isolates of bacteria', Bangladesh J. Life Sci, 22 (2), pp.65-73 (Accessed: 28 March 2022).

Viswanathan, B. (2018) 'Photocatalytic Degradation of Dyes: An Overview', Current Catalysis, 7(2), pp.99-121. [Online] DOI: 10.2174/2211544707666171219161846 (Accessed: 3 April 2022).

Wang, L., Hu, C. and Shao, L. (2017) 'The antimicrobial activity of nanoparticles: present situation and prospects for the future', International Journal of Nanomedicine, Volume 12, pp.1227-1249. [Online] DOI: 10.2147/IJN.S121956 (Accessed: 17 July 2022).

Weerasingha, W., Chandrasiri, M., Hewawitharana, K. and Sampath, J. (2021) 'Evaluation of anthocyanin extracted from Hibiscus rosa-sinensis as a natural food colorant', 10th Annual Science Research Session, FAS, SEUSL, pp.17-20. [Online] Available at: http://ir.lib.seu.ac.lk/bitstream/123456789/5861/1/ASRS2021_Proceedings%20Book-pp.17-20 (Accessed: 10 July 2022).

Wu, L., Liu, X., Lv, G., Zhu, R., Tian, L., Liu, M., Li, Y., Rao, W., Liu, T. and Liao, L. (2021 'Study on the adsorption properties of methyl orange by natural one-dimensional nano-mineral materials with different structures', Scientific Reports, 11(1). [Online] DOI: 10.1038/s41598-021-90235-1 (Accessed: 12 July 2022).

Zehiroglu, C. and Ozturk Sarikaya, S. (2019) 'The importance of antioxidants and place in today's scientific and technological studies' , Journal of Food Science and Technology, 56(11), pp.4757-4774. [Online] DOI: 10.1007/s13197-019-03952-x (Accessed: 29 March 2022).

Zhang, D., Ma, X., Gu, Y., Huang, H. and Zhang, G. (2020) 'Green Synthesis of Metallic Nanoparticles and Their Potential Applications to Treat Cancer', Frontiers in Chemistry, 8. [Online] DOI: 10.3389/fchem.2020.00799 (Accessed: 13 July 2022).

Zhang, X., Liu, Z., Shen, W. and Gurunathan, S. (2016) 'Silver Nanoparticles: Synthesis, Characterization, Properties, Applications, and Therapeutic Approaches', International Journal of Molecular Sciences, 17(9), p.1534. [Online] DOI: 10.3390/ijms17091534 (Accessed: 16 July 2022).

Zhu, X., Pathakoti, K. and Hwang, H. (2019) 'Green synthesis of titanium dioxide and zinc oxide nanoparticles and their usage for antimicrobial applications and environmental remediation', Green Synthesis, Characterization and Applications of Nanoparticles, pp.223-263. [Online] DOI: 10.1016/B978-0-08-102579-6.00010-1 (Accessed: 5 July 2022).